Insar analysis of the effects of the Izmit earthquake with ERS data

F. Sarti[1], F.Adragna[1],N.Pourthié[1],B.Rosich[2],A.Arnaud[2] , K.Feigl[3], M.Rosengren[4] , P.Imbo[5] , D.Petit[6]

[1]CNES, QTIS/SR,
18 avenue Edouard Belin, Bpi 811, 31401 Toulouse, France
Tel : 33.5.61.28.21.33 / Fax : 33.5.61.31.67 / e-mail: francesco.sarti@cnes.fr

[2] ESA/ESRIN
Via Galileo Galilei, 0004 Frascati , Italy
e-mail: brosich@esrin.esa.it

[3] OMP/CNRS
16 Avenue Edouard Belin, 31401 Toulouse, France
e-mail: kurt.feigl@cnes.fr

[4] ESA/ESOC
R. Bosch Str.5, Darmstadt, Germany
e-mail: mrosengr@esoc.esa.de

[5]CESBIO,
18 avenue Edouard Belin, Bpi 2801, 31401 Toulouse, France
e-mail: imbo@cesbio.cnes.fr

[6]IRIT/UPS,
118 Route de Narbonne, 31062 Toulouse, France
e-mail: petit@irit.fr

Abstract

After the 17/08/99 earthquake in Turkey, ESA and CNES decided to coordinate their efforts for the emergency study of the earthquake effects based on satellite observations (ERS, SPOT). In particular, a set of archived ERS acquisitions over the interested sites was promptly provided by ESA, a series of tandem acquisitions were programmed (ERS-1 was switched on over Turkey) and the acquired post-event images were also made available. This allows not only for the study of the first seismic effects, but also for the evaluation and monitoring of the post-seismic deformations. For the particular case of the ERS-1 and ERS-2 orbits 30 and 31 days after the first earthquake, the orbit control strategy could exceptionally take into account InSAR requirements, obtaining minimal orbital baselines between co-seismic interferometric acquisitions over the site of interest.
This paper will present part of the interferometric results obtained at CNES and ESA, using the best available dataset. Several interferograms are compared in order to take into account possible residual topographic effects, and analyse the effect of orbital errors or possible atmospheric artifacts. Further analyses based on different techniques are still ongoing at CNES, such as correlation of optical data and radar multitemporal analysis.

1. Introduction

In the last decade the Radar Department of CNES has contributed to several studies for disaster monitoring, including cartography of earthquake and volcano deformations, measurement of ground subsidences and monitoring of natural or industrial risks based on the CNES differential interferometry tool (DIAPASON) using spaceborne SAR data. SAR differential interferometry allows for the determination of ground displacements with a centimeter level accuracy. The feasibility of deformation mapping based on radar interferometric techniques was well demonstrated at CNES in the case of several earthquakes, including Landers (see for example[1], [2], [3], [4], [5], [6]) and Etna eruptions [7] or, more recently, for the Piton de la Fournaise (La Reunion Island) eruption [8].

On 22nd July at the United Nations UNISPACE III conference in Vienna, ESA and CNES pledged to pool their satellite-based resources and provide timely, pertinent information on parts of the Earth struck by natural or man-made disasters. Less than a month after, on 17 August 1999, a strong earthquake (magnitude of 7.8) shook northwestern Turkey. ESA decided then to initiate an ERS1-ERS2 campaign over Izmit area while CNES started a collection and analysis of multisource (radar/optical) data over the same area.

Radar and optical satellites provide images for Turkey disaster relief operations, with different timescale and space resolutions. Images of the earthquake-struck regions of Turkey are being provided by European observation satellites: ESA's ERS satellites and SPOT satellites of the French national space agency CNES. SPOT 4 yielded detailed pictures of the Izmit and Istanbul areas for 9th July and 20th August, while a large dataset of ERS acquisitions on the area was provided by ESA. Several cloud-free acquisitions acquired by VEGETATION (a large field-of-view optical instrument on the SPOT4 platform providing daily revisit at our latitudes) were also available, including an acquisition taken a few hours after the earthquake.

2. Overview of the region: the North Anatolian fault

The North Anatolian Fault splays westward into two main branches, 100 km apart. The Northern branch bounds the southern side of the Gulf of Izmit, outlines the Marmara pull apart basin, cuts the Dardanelles structure, and marks the southern side of the Saros Gulf. The Izmit earthquake occurred on that branch, east of Marmara Sea.

Geological studies over a longer time period (holocene) indicate a slip rate of 2.5 cm/year on the North Anatolian Fault (Hubert, 1998). The Izmit earthquake broke a 110 km long section of the North Anatolian fault (Armijo et al., more details on the web : http://www.ipgp.jussieu.fr/depts/TECTO./IzmitWEB/IzmitUK.html)

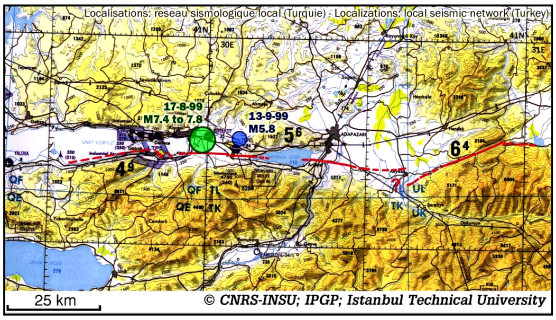

Fig 1: Localization of the local seismic network (Turkey)

3. First interferometric result

The first co-seismic interferogram over the Gölcük area could be generated after the ERS-1 acquisition of the 25th August 1999. This interferogram was computed at CNES using this ERS-1 acquisition (25th August, orbit 42408) and the ERS-2 image acquired on 24 December 1998 (orbit:19228) on an ascending track 336 (Fig.2). This first interferogram was available at the beginning of September. In spite of a baseline favourable to differential interferometry (about 40 m) a poor coherence was obtained because of the 8 month interval.

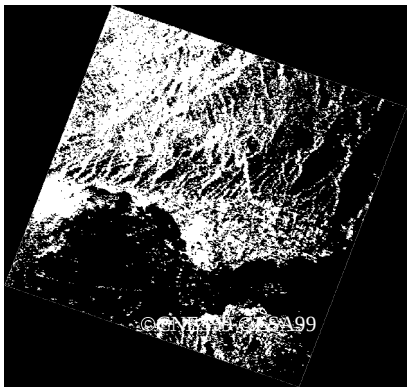

Fig. 2: Extract of the first CNES interferometric result (ERS-2 24/12/98 - ERS-1 25/08/99). It showed poor coherence, limited to the zone northern of Derince.

The next acquisition over the track 336 (26th Aug.) had a long baseline with the pre-event acquisitions, resulting in a too large frequency shift in range and in a limited coherency. Following acquisitions (10th/11th Sept., track 64) had also long baseline with the corresponding pre-earthquake images.

4. Orbit control

On factor limiting the accuracy of the interferometric results depends on the separation of the two orbits at the acquisition time: the smaller the separation, the lower the sensitivity to topography and to DEM residual errors. Fig.3 shows the perpendicular baseline between the two ERS-2 orbits computed over the subsatellite point of coordinates 26.54 E (longitude), 40.63 N (latitude). The orbital baseline relative to Izmit was about 18 m, corresponding to 566 m altitude of ambiguity.

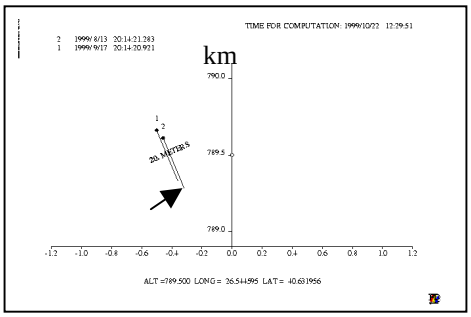

Figure 3: Perpendicular baseline computed by ESA/ESOC between two ERS-2 orbits (22556 and 23057) which allowed high quality interferogram on the Izmit area.

Without adapting the orbital manoeuvre strategy the baseline would have been 40 times larger (800 m) and the high quality interferogram shown on *Fig.4* would not have been possible, because of reduced coherency. These computations allowed ESA to pilot ERS orbits in order to optimize differential interferometry performances, without disturbing other users, for the particular case of the ERS-2 23057 orbit (with ERS-2 22556 as a reference orbit). The main orbit maintenance manoeuvre (that would have been needed anyway) was slightly anticipated to September 14th, 1999 with one burn at 3:47 Z and one burn at 4:37 Z. This was a few days earlier than it would have been the case without the "Izmit project" and this time was selected to have a minimal baseline at Izmit. A small "touch-up" manoeuvre had to be executed on September 15th, 1999 at 0:51 Z to compensate for the manoeuvre dispersion and two small "touch-up" manoeuvres had to be executed 99/09/16 at 0:51 Z and 23:20 Z to compensate for the unexpected low air-drag (relative to the available air-drag model). If the main orbit maintenance manoeuvre would have been executed 2 days later the Izmit baseline would have been in the order of 700 - 800 m. The orbit control strategy and precise orbit determination were performed at ESA/ESOC, Darmstadt. More details on ERS orbital control at ESOC are available on the web page: http://nng.esoc.esa.de

5. Best interferometric result

The pair ERS-2 23057-ERS-2 22556, with a 35-days interval, descending track, with a dedicated orbital control strategy allowed for an excellent altitude of ambiguity and a good interferometric coherence. Radar synthesis and interferometric processing were performed by the Radar System Department of CNES, using the Diapason software. ESA restituted orbits were used, and the results were validated using three different DEM with a 100 m grid (the re-sampled GTOPO30, a commercial DEM derived from digitized maps, a tandem interferometric DEM that was kindly made available by the university of Oxford). The large altitude of ambiguity and the almost identical results in the three cases guarantee that the interferogram did not contain residual topographical effects.

Fig.4 shows ground deformation due to the 17 August 1999 earthquake in the region of Izmit, Turkey. This representation is obtained by super-imposing an ERS radar image (Fig.5) to the image of the measured deformations (Fig.6).

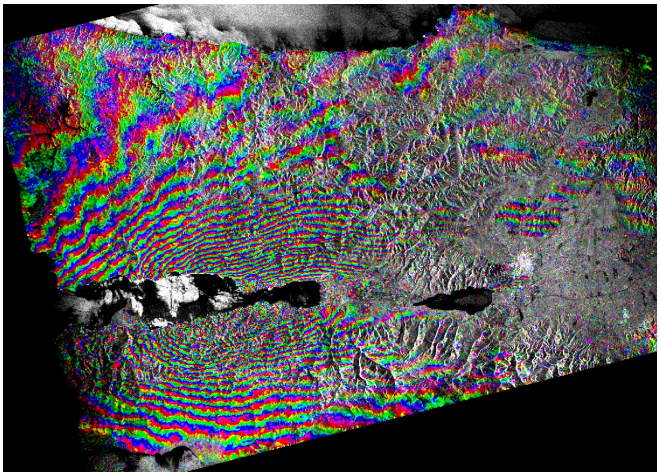

Fig.4 : superimposition of the amplitude image and the phase interferogram (ERS-2 13/08/99 - ERS-2 17/09/99)

Each colour cycle corresponds to a 28-mm change in distance between the ground and the satellite. A geophysical deformation model is described in par.7.

Radar image analysis provides an intensity measure as well as a phase information (radar wave travel time) at each point. *Phase* is directly related to the distance between the observed target and the radar. By computing phase differences between two satellite acquisitions, it is possible to measure ground displacement during the time interval elapsed between acquisitions, with a centimeter-level accuracy.

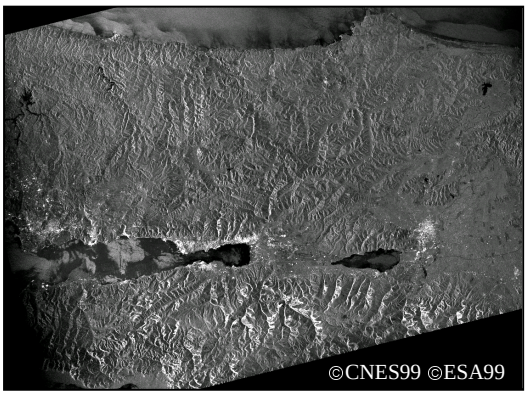

Fig.5: Mean Amplitude Image (ERS-2 13/08/99 - ERS-2 17/09/99)

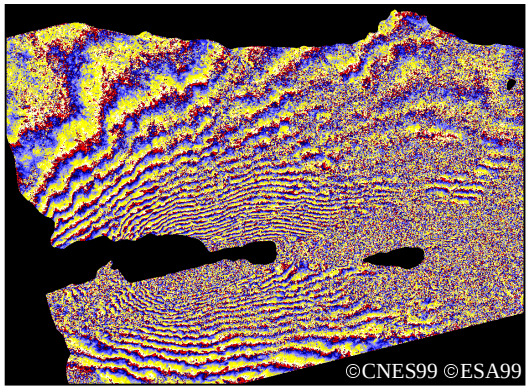

Fig.6: Phase Interferogram (ERS-2 13/08/99 - ERS-2 17/09/99)

The first satellite image for this pair was acquired by the ESA satellite ERS-2 over Izmit on 13/08/99, four days before the earthquake, from an altitude of 800 km. The second image was programmed and acquired on 17/09/99, one month after the earthquake. This interferogram was compared to the ERS-1 12/08/99-ERS-1 16/09/99 interferogram (respectively in tandem configuration with the two ERS-2 acquisitions used previously). This ERS-1 interferogram was slightly less coherent than the ERS-2 interferogram shown in Fig. 4, but it allowed to validate this result and to ensure that the observed fringes were free of atmospheric effects.

6. Impact of precise orbits

ERS predicted orbits are first estimated at ESOC 6 days before the pass, then 3 days before and finally 1 day before. The accuracy of predicted orbits depends on solar activity, which was very high in '91 and will reach its maximum in 2001. Accuracy in orbit estimation 6 days before the orbital pass can then vary from about 100 m (like in August '96) to 2 km (in a period of high solar activity, like Feb'99). Predicted orbits are used to adjust the orbit control manœuvres.

The interferogram shown in par.5 was first obtained using the restitued orbits computed by ESOC. These orbits are available et ESOC 1-2 days after the satellite pass. They are estimated to be 1-2 meters rms accurate in cross-track, 2-4 meters rms in along-track about 50 cm rms in the radial component.

ERS precise orbits are estimated at ESOC 7-10 days after the orbit pass and are the result of a least square estimation based on Laser and Radar altimeter data collected over 4 days and including accurate orbital and perturbation models. The accuracy of precise orbit estimation is of the order of 20-30 cm rms (along-track, cross-track components), 10 cm rms (radial component). Their accuracy is similar to that of precise orbits computed by Delft or by DLR.

The interferogram shown in Fig.4 was recomputed using these precise orbits, and the difference with respect to the previous interferogram is shown in Fig.7.

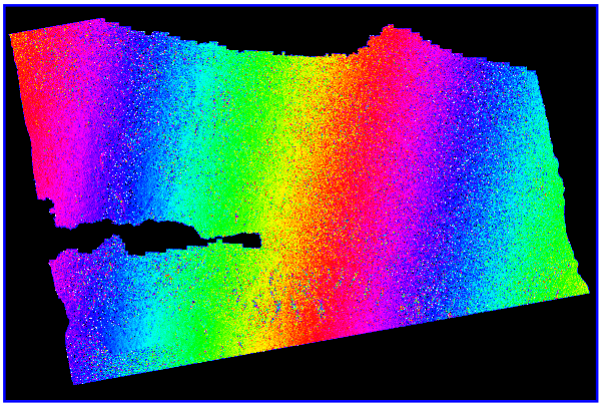

Fig.7: Residual orbital fringes on the ERS-2 13/08/99 - ERS-2 17/09/99 interferogram when passing from restituted to precise orbits

Fig.7 shows that the impact of precise orbits versus restituted orbits is minor for the case of the ERS-2 13/08/99 - ERS-2 17/09/99 interferogram (a few fringes in range, in a case where several tens of displacement fringes in azimuth are observed). The availability of precise orbits may neverthless be important for different cases. More details about ERS orbit determination at ESOC are available on the web page http://nng.esoc.esa.de

7. Geophysical model and orbital cleaning

The geometry of the fault rupture and the measured deformations allow the geophysicists to build a theoretical model of the fringe pattern of the seism. Some examples were shown in [9],[10]. One of these geophysical models for Izmit was produced by K.Feigl, OMP/CNRS (Fig.8)

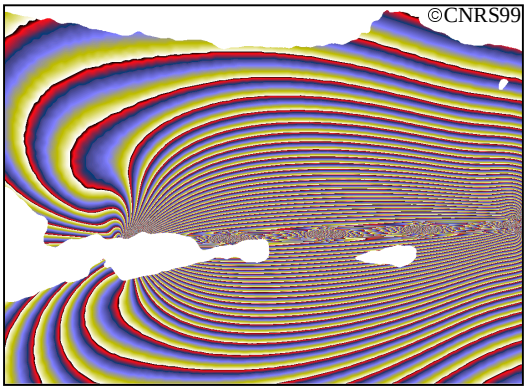

Fig.8: A theoretical model simulating the fringe pattern produced

This model is estimated by nonlinear inversion of the manually unwrapped fringes. It was also assumed that the absolute fringe counts on the north and south sides are offset according to the profile of Fig.9. This model assumes 4.3 meters of right-lateral slip on a fault 78 km long and 15 km wide which cuts the surface vertically and strikes at an azimuth of 85 degrees. This is equivalent to magnitude 7.48. The calculation assumes the conventional dislocation in an elastic half space.

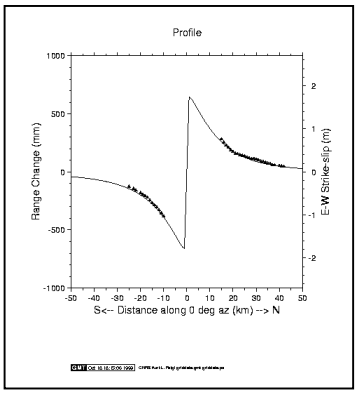

Fig.9: Profile of the computed model simulating the fringe pattern.

Profile extending from south to north through the maximum number of fringes. To perform the orbital correction, we assumed that the fringe gradient must be symmetric about the fault, located at the origin of this profile (0 km). This assumption is justified by the elastic half space calculation (solid line). We adjust the fringe pattern accordingly by adding a north-south gradient (number of fringes per km), or 10 fringes over the length of the image. The necessity for this assumption would be alleviated by either a longer data acquision or more precise orbits.

The geophysical interpretation of the observed fringes is that a vertical, east-west trending fault ruptured in with right-lateral strike slip of over 4 meters. Assuming purely horizontal, east-west motion, we find that one fringe of range change implies 66 mm of displacement. This displacement is eastward north of the fault (and the bay), and westward to the south. The fringes closing near the west edge of the peninsula suggests that the rupture terminates near the triangular delta.

This theoretical model and the orbital cleaning will be improved using in-situ data which are now becoming available, longer data records (orbital fringes in azimuth) and precise orbits (orbital fringes in range)

8. Comparison with optical data

ERS interferograms can be combined with optical data such as SPOT multitemporal observations that provide a useful complementary local information. Two days after the earthquake, Spot Image promptly reacted by programming the SPOT satellites over the disaster area. On the 20th of August, SPOT 4 acquired the first image that fortunately was cloud-free.
20 images in total where acquired in 23 days by SPOT (16 with SPOT 4). Only 8 acquisitions were exploitable because of the meteorological conditions. Two cloud-free acquisitions of SPOT4, before and after the earthquake, were compared and superimposed, in order to detect variations due to earthquake effects.

Fig.10 shows a zoom of the two acquisitions, close to the harbour of Gölcük. Flooded areas due to earthquake-induced subsidence can be observed.

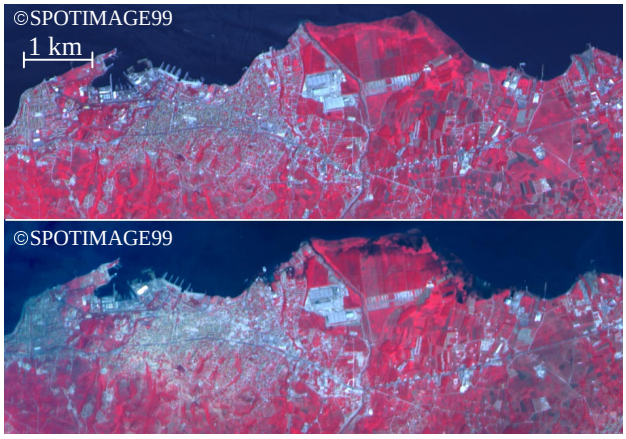

Fig.10: Extracts of SPOT 4 XS acquisitions over Gölcük. Top: 09/07/99 Bottom: 20/08/99

Fig. 11 and 12 are obtained superimposing the acquisition of the 9th of July (before the earthquake) to the one of the 20th of August. This colored composition of multitemporal acquisitions allows for the localisation of visual changes such as fires or areas underwater. Fig.11 shows clearly the subsidence (vertical deformation component) on the area of Gölcük : the two

red areas along the coastline indicate changes due probably to a bradyseism phenomenon. The large red area in Fig.12, on the south of Derince, is due to the smoke plume of a fired refinery.

Fig.11: Superimposition of two Spot 4 images (before and after the earthquake) over the harbour of Gölcück)

Fig.12: Superimposition of two Spot 4 images (09/07/99 and 20/08/99) over the south of Derince. Red is associated to the image acquired after the earthquake is colored in red, Green and Blue to the pre-seismic image.

Several cloud-free acquisitions taken by VEGETATION (a large field-of-view optical instrument on the SPOT4 platform) were available, including an acquisition taken a few hours after the earthquake was also available. Though with a resolution (1 km) not adapted to the study of the effects of the Izmit earthquake, this instrument shows a good potential for other applications of global monitoring or major floods/fires, because of its daily revisit at our latitudes.

Correlation results using radar intensity images or optical (Spot) data may also give very useful complementary information on the fault rupture, where interferometric fringes become too dense and coherence decreases.

9. Conclusions and perspectives

In-situ data are now becoming available and allow for a model validation and improvement. Together with an utilisation of longer data records containing southern frames, they will allow for a more precise correction of orbital effects.

We also envisage to perform a fusion with the results derived from optical analysis, and from radar or optical correlation.

Radar multitemporal analyses are also planned at CNES in order to perform a study of damaged urban areas.

This work is an example of a successful collaboration between several space agencies and research centers, sharing available data, human resources, expertise and processing resources in order to promptly put at the disposal of the scientific community the results of space observations for the monitoring of natural disasters.

10. Acknowledgments

We thank ESA/ESRIN for promptly providing the data, ESA/ESOC for the details about orbit determination and control, SPOT IMAGE for the SPOT4 data. We are grateful as well to all the contributors of the multi-disciplinary work described in this paper. Special thanks to J.Dow (ESA/ESOC), P.Durand (CNES/QTIS), E.Fielding (JPL/University of Oxford), D.Massonnet (CNES/QTIS), M.Barbieri, L.Castellano, N.Walker (SERCO), R.Gachet and P.Tissier (CNES/QTIS), H.Joannes and L.Demargne (SPOT Image).

11. References

[1] D. Massonnet, M. Rossi, C. Carmona, F. Adragna, G. Peltzer, K.L. Feigl, and Th. Rabaute, "The displacement field of the Landers earthquake mapped by radar interferometry", Nature, vol. 364, pp. 138-142, July 1993

[2] D. Massonnet, K.L. Feigl, M. Rossi, and F. Adragna "Radar interferometric mapping of deformation in the year after the Landers earthquake", Nature, vol. 369, 227-230, 1994a.

[3] D. Massonnet, K.L. Feigl, H. Vadon, and M. Rossi, "Coseismic deformation field of the M = 6.7 Northridge, California, earthquake of january 17, 1994, recorded by two radar satellites using interferometry", Geophys. Res. Lett., vol. 23, pp. 969-972, 1996a.

[4] D. Massonnet, W. Thatcher, and H. Vadon, "Detection of postseismic fault zone collapse following the Landers earthquake", Nature, vol. 382, pp. 612-616, 1996b.

[5] B. Meyer, R. Armijo, D. Massonnet, J.B. Chabalier, C. Delacourt, J.C. Ruegg, J. Achache, P. Briole, and D. Panastassiou, "The 1995 Grevena (northern Greece) earthquake: Fault model constrained with tectonic observations and SAR interferometry", Geophys. Res. Lett., vol. 23, pp. 2677-2680, 1996.

[6] D. Massonnet, and K.L Feigl, "Satellite radar interferometric map of the coseismic deformation field of th M = 6.1 Eureka Valley, California, earthquake of May 17, 1993", Geophys. Res. Lett., vol. 22, pp. 1541-1544, 1995b.

[7] D.Massonnet, P. Briole, and A. Arnaud, "Deflation of Mount Etna monitored by spaceborne radar interferometry", Nature, vol. 375, pp. 567-570, June 1995.

[8] F. Sigmundsson, Ph. Durand, and D. Massonnet, "Opening of an eruptive fissure and seaward displacement at Piton de la Fournaise volcano measured by RADARSAT satellite radar interferometry", Geophys. Res. Lett., vol. 26-5, pp. 533-536, March 1999.

[9] K.L. Feigl, A. Sergent, and D. Jacq, "Estimation of an earthquake focal mechanism from a satellite radar interfergram: Application to the December 4, 1992, Landers after-shock", Geophys. Res. Lett., vol 22, pp. 1037-1048, 1995.

[10] D. Massonnet, and K. Feigl, "Discrimination of geophysical phenomena in satellite radar interferograms", Geophys. Res. Lett., vol. 22, pp. 1537-1540, 1995.